



Contents lists available at ScienceDirect

Sensing and Bio-Sensing Research

journal homepage: www.elsevier.com/locate/sbsr

Development of Si-based electrical biosensors: Simulations and first experimental results



Marco Favetta^a, Antonio Valletta^b, Guglielmo Fortunato^b, Maria Eloisa Castagna^c, Sabrina Conoci^c, Emanuele Luigi Sciuto^d, Tiziana Cosentino^e, Fulvia Sinatra^e, Sebania Libertino^{a,*}

^a CNR-IMM, Strada VIII Z.I. n. 5, 95121 Catania, Italy

^b CNR-IMM UOS Roma, via fosso del cavaliere n. 100, 00133 Roma, Italy

^c STMicroelectronics, Strada Primosole n. 50, 95121 Catania, Italy

^d Dept. of Physics, University of Catania, via Santa Sofia n. 64, 95123 Catania, Italy

^e Dept. of Biomedical and Biotechnological Sciences, University of Catania, via Santa Sofia n. 87, 95123 Catania, Italy

ARTICLE INFO

Article history:

Received 25 September 2015

Received in revised form 23 November 2015

Accepted 25 November 2015

ABSTRACT

In this work, we simulated and experimentally assessed the possibility to detect, through electrical transduction, hybridization of DNA molecules on MOS-like devices, having different dielectrics: SiO₂, Si₃N₄ and SiO₂/Si₃N₄/SiO₂ (ONO). The electrical characterization was performed after the various functionalization steps, consisting of dielectric activation, silanization, DNA spotting and anchoring, and after the hybridization process, to test the devices effectiveness as DNA recognition biosensors. The experimental results were used to validate device simulations. The comparison shows the ability to determine a priori the DNA probe density needed to maximize the response. The results confirm that the structures analyzed are sensitive to the immobilization of DNA and its hybridization.

© 2015 Published by Elsevier B.V. This is an open access article under the CC BY-NC-ND license (<http://creativecommons.org/licenses/by-nc-nd/4.0/>).

1. Introduction

In the last 20 years, there has been a wide interest to the development of integrated and miniaturized biosensors fabricated with industrial processes to allow mass production. To this purpose, there is a growing interest in creating micro-biosensors fabricated on Si-based technology. Such technology could provide several advantages: small size and low weight, fast response, device's analytical performance improvement and accuracy of the analysis, high reliability, low energy consumption, possibility of automatic packaging, on-chip integration of biosensors' arrays, and low-cost-mass production of portable microanalysis systems [1].

For Si-based micro-biosensors the identification of an efficient transduction mechanism plays an essential role. The most used transduction mechanisms in biosensors are: optical (indirect method) [2] and electrical (direct method) [3]. The first is the most used method in DNA-chip applications [4,5] and is fully accepted by the biomedical community. It lays on the ability to detect a signal from a labeled target molecule rather than from the molecule itself. It is generally characterized by expensive and unwieldy lab equipment [4], therefore, in-situ measures or portable/disposable detectors are not available up to now. Moreover, image-processing analyses for automatic detection are required and

software for post processing is needed. Also using a smaller device and/or system [6], a labeling step before the detection is required.

Electrical transduction would provide several advantages in terms of realization of simple, portable and inexpensive sensors [3]. It is based on the monitoring of the surface modifications upon biomolecular reactions. Therefore, it could provide a valid alternative to optical methods for detecting DNA hybridization or similar molecular recognition events. Several new approaches for the direct reading of label-free DNA have been proposed in recent years [7,8]. Microelectronic devices could play a key role in this area, thanks to the high repeatability and precision of the response, their easy use and control, and their well-established technologies. One of the main advantages of this kind of devices is their ability to detect target molecules not labeled. In this way, they overcome errors due to the link of enzymatic labels, occurring in some microarray techniques [9] and strongly reduce the sample preparation.

Among the different devices proposed in literature, some use the variation of redox reactions during hybridization as operation principle. Other devices detect the variation of a capacitance in a double layer after the hybridization [7]. Those based on the variation of the surface potential are the ion sensitive field effect transistors (ISFET) [10]. They are able to detect the intrinsic charge of a molecule adsorbed on the sensor surface. The ISFET working principle is the measure of a threshold voltage (V_{th}), or drain current (I_d), variation, due to the DNA charge presence on the gate. ISFET biosensors would benefit of the typical

* Corresponding author.

transistor efficiency and effectiveness, especially for their integration in microelectronics production lines, thus allowing low costs and large-scale production.

The technology used in this work is based on electrolyte–insulator–semiconductor (EIS) biosensors. EIS vary their potential because of a detection event at the insulator/electrolyte interface. For this structure, capacitance vs voltage (CV) measurements provide information on the interface potential [11]. The chemical changes that take place at this surface, such as the immobilization of biological molecules, or hybridization of a molecule of single strand DNA (ss-DNA, probe) with the complementary strand (target), will cause a potential variation, measured as a shift of the CV curve. The shift sign and amplitude will depend on the nature and coverage of material modification.

The device capacitance is given by the series of three main capacitors: i) the semiconductor/insulator ($C_{S/I}$) given by the “inorganic” part of device; ii) the biological sensing molecule (our probe) (C_{probe}); and iii) the region spanning from the outer device surface and the bulk of the solution (C_{int}). C_{probe} includes the Stern layer consisting of electrostatically bound water molecules between the recognition and diffuse layers and, eventually, the recognized analyte [12]. The total capacitance C_{tot} , is then:

$$\frac{1}{C_{tot}} = \frac{1}{C_{S/I}} + \frac{1}{C_{probe}} + \frac{1}{C_{int}}. \quad (1)$$

The equation clearly states that the lowest capacitance dominates the total capacitance. Therefore, for the device design the tradeoff between the need to have a high insulating layer capacitance to lower its contribution (high oxide thickness), and the need to have a high sensitivity, hence a thin oxide, is important. The recognition event will change C_{probe} value. The capacitance variation can be quantified by monitoring the voltage shift.

Aim of this work is to verify the possibility of using different MOS-like devices as biosensors for the detection of the hybridization processes of probe DNA, and to study their electrical response.

2. Materials and method

Three different dielectrics were thermally grown, on p-type epitaxial Si wafers having a resistivity of the epi layer of $\sim 2 \Omega \text{ cm}$, a thickness of $7 \mu\text{m}$, grown on CZ Si with a resistivity of $\sim 2 \text{ m}\Omega \text{ cm}$ to fabricate MOS-like structures. The dielectrics were:

- silicon oxide, 85 nm thick;
- silicon nitride, 70 nm thick;
- a multilayer of $\text{SiO}_2/\text{Si}_3\text{N}_4/\text{SiO}_2$ having thickness of 10/20/10 nm ($\sim 30 \text{ nm}$ of equivalent thickness).

Each support underwent the various phases of probe immobilization, consisting of: oxide cleaning and activation; silanization using 3-glycidioxypropyltrimethoxysilane (GOPS); polymerization; deposition and immobilization of biological molecules in localized region of sample (anchoring of oligonucleotide-DNA); stabilization of the surface through bovine serum albumin (BSA). The immobilization process, optimized by STMICROelectronics, is fully described in [12,13].

The DNA sequence used is the following: AGTGAGGGAGGAGATGGA ACCATCT.

Electrical characterization was performed after each functionalization step for all the dielectrics used. The samples were measured using a Wentworth probe station and a capacitance meter (Agilent, model E4980A), applying voltages ranging from -2 V to $+8 \text{ V}$, with frequencies in the range 100 Hz – 1 MHz . A mini chamber was realized on the sample surface by using a glass having a conductive layer of indium tin oxide (ITO, Sigma-Aldrich with $8 \div 12 \Omega/\text{sq}$ surface resistivity) glued on the surface through a spacer with a hole of 4 mm of diameter. A drop of Phosphate-buffered saline (PBS) solution

at 1 M concentration was deposited within the chamber before sealing. An Al foil, inserted between the spacer and the ITO layer, ensures the upper electric contact. The results, shown in the following sections, refer to a sampling frequency of 5 kHz . Our results indicate that at relatively low frequencies the solution used as upper electrode does not affect the measurements. The solution presence does affect the measurements for frequencies above 100 kHz in our configuration. Higher frequencies may be used reducing the solution thickness.

3. Results and discussions

The immobilization protocol effects on the device active surface were electrically characterized using the structure described in the previous section. Fig. 1 shows the comparison of the CV curves acquired for the sample Si/SiO_2 after each immobilization step.

Fig. 1 clearly indicates that the device is sensitive to a charge variation on its surface, as already observed in literature [14,15]. Indeed, after the silanization process, a net positive charge is anchored to the surface, as observed by the CV curve (blue dashed line), that exhibits a shift of $\sim -0.60 \text{ V}$ (left shift) with respect to the reference sample (SiO_2 , red dotted curve). Furthermore, the negative charge introduced by the ss-DNA used as a probe (anchoring phase, green solid line) produces a positive shift with respect to the reference of $\sim +0.20 \text{ V}$. The full shift measured with respect to the step before anchoring is of $\sim 0.8 \text{ V}$.

The C_{min}/C_{ox} values are roughly the same, ~ 0.32 for each curve. The flat band voltage (V_{fb}) values vary according to the surface transformation process of the sample, showing the measurement technique sensitivity to the potential variations on the surface. These results indicate that the CV curves shift can be valid system to detect DNA hybridization and can be used as transduction mechanism in biosensors. Finally, the BSA processing time does not produce detectable variations in the CV measurements.

The measurements reported in Fig. 2 provide other interesting information. The BSA passivation of the surface, widely used in optical biosensors to reduce the artifacts, does not produce significant variation in the electrical measurements. BSA, under the experimental condition used (PBS pH 7.4) does not improve the electrical device sensitivity between the anchoring and hybridization phases. Indeed, the measured shift between the curves of samples having only the probe anchored (blue dotted line) and after hybridization (light blue solid line) without BSA passivation of the surface is $\Delta V \sim 0.60 \text{ V}$, while between the curves with BSA (green dashed line and magenta dash dotted line for probe anchoring and hybridized samples, respectively) it is $\Delta V \sim 0.40 \text{ V}$.

If an effect can be evidenced, it is detrimental to the device operation. In fact, the system is less sensitive and, if the standard deviation is considered (dot-dashed lines in Fig. 3), the two curves obtained by probe anchoring and perfect match hybridization almost overlap. The results show that in these conditions there is not enough confidence to detect DNA hybridization.

Therefore, for our MOS-like systems, we focused on samples without BSA passivation. Fig. 4 shows the Si/SiO_2 samples already described in Fig. 2 including their standard deviations (dot-dashed green lines). The shift of $\sim 0.60 \text{ V}$ after hybridization is clearly wider than the errors; hence, it is a good measure the detection of DNA hybridization.

When the voltage variation is applied to the gate of a MOSFET biased under threshold, an increased drain current up to three orders of magnitude is achieved.

3.1. MOS-like simulation

We developed a 2D simulation of our devices using the commercial software Sentaurus®. Through Sentaurus, we simulated the device functionalization (ssDNA anchoring) and perfect match hybridization by varying the charge density at the interface of the oxide and the “metallization” of our MOS-like device. To simplify the simulation we

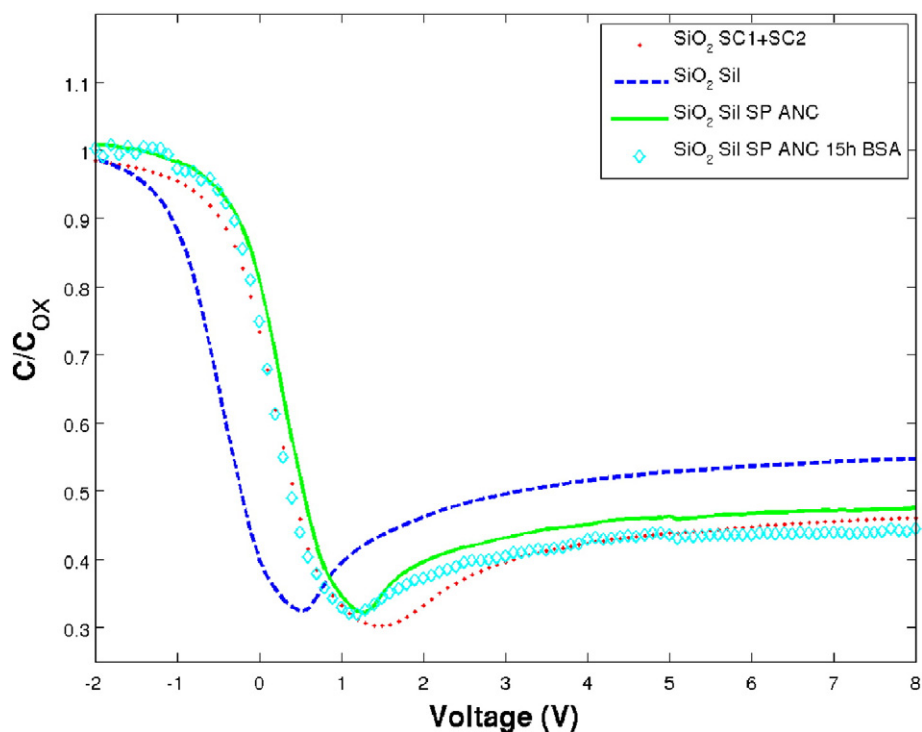


Fig. 1. CV curves of samples having SiO_2 as dielectric, acquired at a frequency of 5 kHz, for the processing steps of: oxide activation (red dotted line), silanization (blue dashed line), anchoring (green solid line) and anchoring + 15 h BSA deposition (light blue diamond line).

assumed the solution and ITO layers as a single metal layer. Fig. 5 reports the CV curves obtained by simulation as a function of the electron density at the interface. The curves are relative to three different electron densities: 0 (reference sample), $2 \times 10^{12} \text{ e}^-/\text{cm}^2$, and $4 \times 10^{12} \text{ e}^-/\text{cm}^2$. The charge densities correspond, respectively, to

2×10^{11} single strands of DNA having 20 bases and 2×10^{11} double strands of DNA having 40 bases each. The estimation was carried out without considering the solution effects on the total charge. For a charge change of $2 \times 10^{12} \text{ e}^-/\text{cm}^2$, the CV shifts of $\sim 0.60 \text{ V}$. The simulation data perfectly match the experimental results, if we assume that the

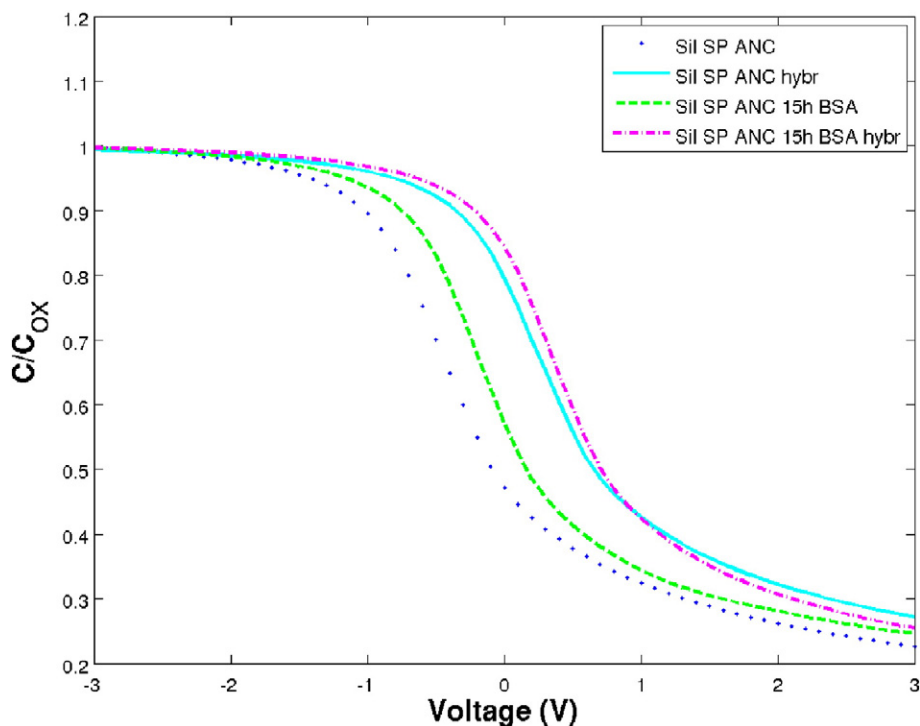


Fig. 2. CV curves of samples that underwent ssDNA anchoring with (green dotted line) and without (blue solid line) BSA passivation and of the same samples after DNA hybridization (dash-dotted magenta and light blue dashed lines, respectively).

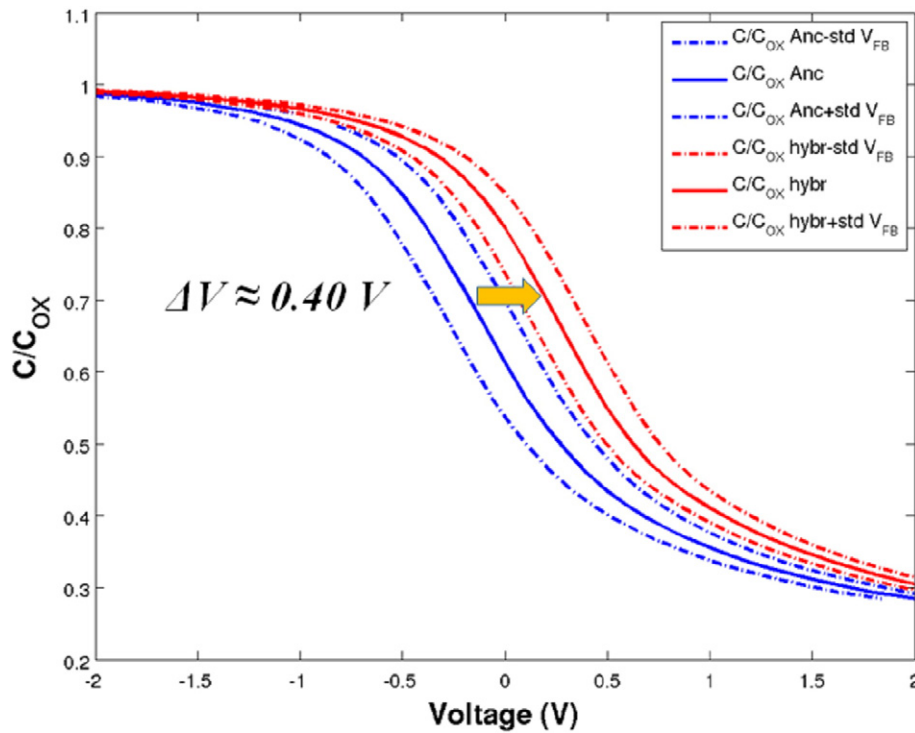


Fig. 3. CV curves of samples that underwent ssDNA anchoring (blue solid line) and perfect match hybridization (red dashed line) with BSA passivation. The dot-dashed lines are the standard deviations of the curves.

charge variation experimentally detected after DNA hybridization is $2 \times 10^{12} \text{ e}^-/\text{cm}^2$. These results allow us to make an a priori estimate of the charge density per unit area, hence to determine the probe density, that our device should have to provide a CV shift $> 0.5 \text{ V}$ between the ssDNA sample and perfect match hybridization.

Under the same assumptions, a 100-mer oligonucleotide will introduce a charge 4 times higher than a 25-mer molecule. It is reasonable to assume that the device sensitivity will increase of a factor 4. For a 400-mer oligonucleotide, the sensitivity will increase by a factor 16. In terms of oligonucleotide density, the same results simulated

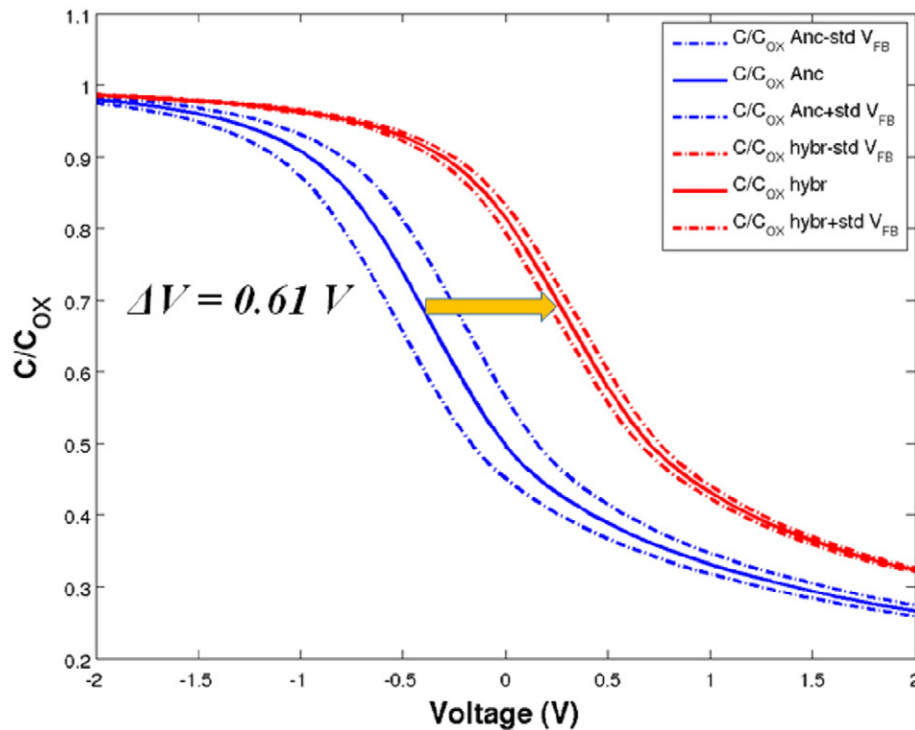


Fig. 4. CV curves of samples that underwent ssDNA anchoring (blue solid line) and perfect match hybridization (red dashed line) without BSA passivation. The dot-dashed lines are the standard deviations of the curves.

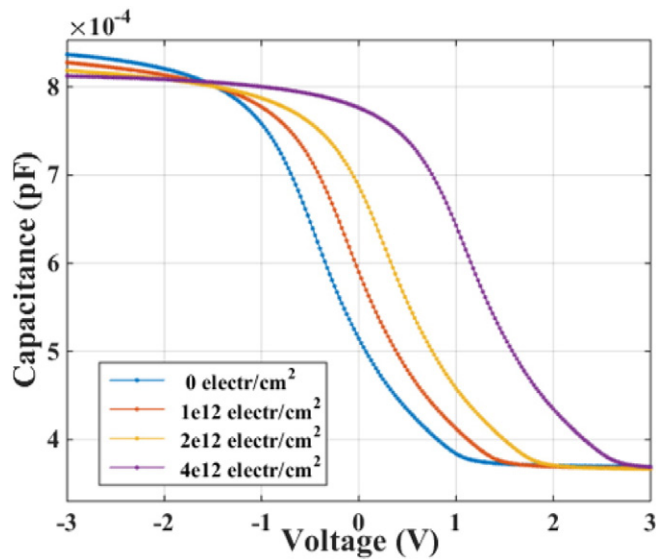


Fig. 5. CV curves simulated with Sentaurus®, for a MOS-like device without charge (blue line), and for an electron densities of $1 \times 10^{12} \text{ e}^-/\text{cm}^2$ (red line), $2 \times 10^{12} \text{ e}^-/\text{cm}^2$ (yellow line) and $4 \times 10^{12} \text{ e}^-/\text{cm}^2$ (violet line).

will be obtained by $\sim 2.5 \times 10^{10}$ oligonucleotides/ cm^2 and $\sim 6.3 \times 10^9$ oligonucleotides/ cm^2 , for 100 and 400 mer oligonucleotides, respectively.

3.2. Comparison among MOS-like diodes having different dielectrics

Finally, we investigated the possibility to use different dielectrics, compatible with microelectronic processing, to fabricate DNA biosensors. In particular, Si_3N_4 and oxide/nitride/oxide (ONO) surfaces were investigated. Fig. 6 reports an example of the results obtained for

ssDNA probe anchoring (blue solid line) and perfect match hybridization (red dashed line) on the $\text{Si}/\text{Si}_3\text{N}_4$ sample.

The nitride on Si sample exhibits the VFB at -5 V . It is due to the positively charged defects lying in the nitride layer, which shift the CV curves towards negative values. The DNA immobilization will cause the shift already observed towards values that are more positive.

The shift of the two curves is lower than the one observed in Si/SiO_2 samples (see Fig. 4). It is probably due to the presence of defects within the dielectric that may shield the DNA charge effect. The defects in the voltage range applied to the samples (-10 V ; -2 V) may capture electric charges causing a modification of the bare material properties that can shield the “external” modifications due to the DNA charge presence. Indeed, the same sample can provide different CV curves, depending on the voltage range used and on the biasing times.

A similar phenomenon was observed also in ONO samples, due to defects present in the nitride layer. Nevertheless, in this dielectric the defect presence is strongly reduced, being confined to 200 nm of nitride layer, and the interface defects is strongly suppressed by the presence of a silicon oxide layer at the interface with the bulk Si. Fig. 7 reports an example of hybridization data on these samples; in fact, the probe anchored sample before and after hybridization are compared.

Also in this case a positive shift of $\sim 0.40 \text{ V}$ of the CV curve after hybridization is observed. Unfortunately, the shift is barely above the errors measured for these samples, similarly to the case already reported in Fig. 3. On the other hand, the ONO samples present an interesting characteristic that may make them interesting. We verified the presence of a “memory” effect in our samples, as already observed on ONO dielectrics [16]. By applying a positive bias voltage, the curve shifts towards positive values. In particular, by filling all the traps in the ONO layer it would be possible to eliminate the defect shielding of the DNA hybridization, already observed in nitride MOS-like samples. Therefore, we verified if the shift process was reproducible and the results are summarized in Fig. 8. We repeated these steps cyclically several times to check if the CV curves shifts are reproducible and depend only on the applied voltage. As shown in Fig. 8, the curves representing “programed” ONO

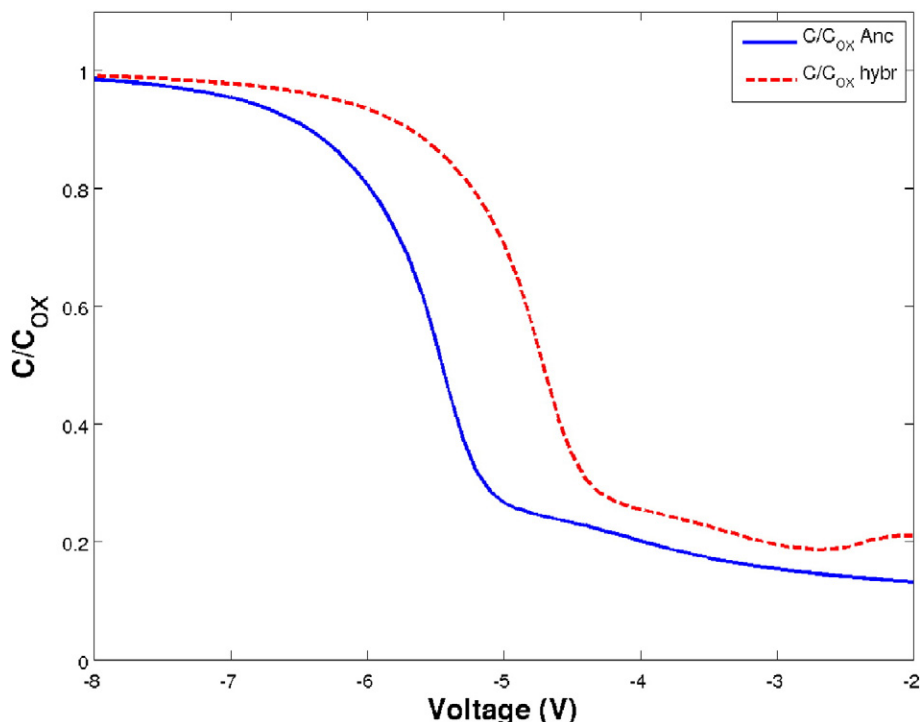


Fig. 6. CV curves for ssDNA probe anchoring (blue solid line) and perfect match hybridization (red dashed line) on the $\text{Si}/\text{Si}_3\text{N}_4$ sample.

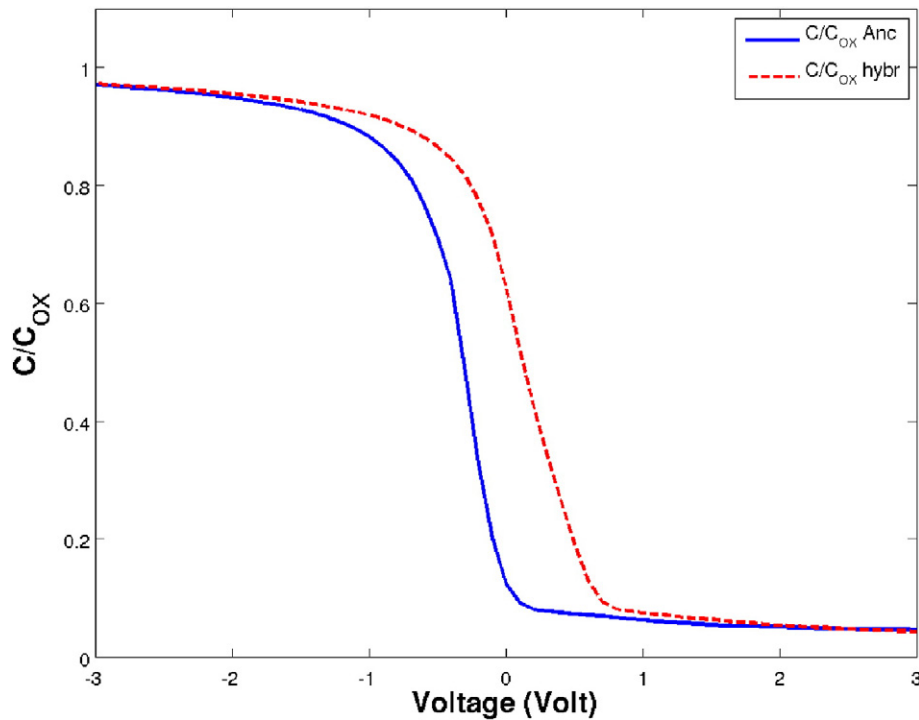


Fig. 7. CV curves for ssDNA probe anchoring (blue solid line) and perfect match hybridization (red dashed line) on the Si/ONO sample.

devices are perfectly reproducible, showing a shift of ~ 2 V with respect to the “erase” condition.

The results shown open interesting possibilities to the use of ONO dielectrics in DNA chip applications.

4. Conclusion

MOS-like sensors for the direct detection of DNA hybridization have been investigated. We studied different dielectrics to detect DNA hybridization in order to define the best in terms of response and

stability. By using SiO_2 as dielectric, a shift of ~ 0.60 V was measured after hybridization, well above the experimental errors. By simulating our devices with the commercial software Sentaurus® we determined that an electron density $\sim 2 \times 10^{12} \text{ e}^-/\text{cm}^2$ produces a shift comparable with the experimental data. The simulation may help us to select, a priori, the DNA probe density on the sensitive area of the device in order to maximize the response.

The other dielectrics studied, based on silicon nitride (Si_3N_4 and ONO), indicate that the trap presence in the nitride layer is detrimental to the device correct operation. Nevertheless, a proper device design, using ONO layers, may allow using the ONO “memory effect” to propose new biosensors for the detection of DNA hybridization.

The development of biosensors based on the electrical transduction of the biochemical signal look promising, thanks to their compatibility with current technologies.

Acknowledgments

This work has been partially funded by the National Project MIUR-PON “Hippocrates – Sviluppo di Micro e Nano – Tecnologie e Sistemi Avanzati per la Salute dell'uomo” (PON02 00355).

We would like to thank Mr. D. Corso per helping in the experiments setup.

References

- [1] R. Davidsson, F. Genin, M. Bengtsson, T. Laurell, Microfluidic biosensing systems. Part I. Development and optimization of enzymatic chemiluminescent μ -biosensors based on silicon microchips, *J. Lab Chip* 4 (2004) 481–487.
- [2] S. Moore, Making chips to probe genes, *IEEE Spectr.* 38 (3) (Mar. 2001) 54–60.
- [3] R. Moeller, W. Fritsche, Chip-based electrical detection of DNA, *Proc. Inst. Elect. Eng. Nanobiotechnol.* 152 (1) (Feb. 2005) 47–51.
- [4] M. Schena, *Microarray Analysis*, John Wiley & Sons, New Jersey, 2003.
- [5] B. Foglieni, A. Brisci, F.S. Biagio, P. Di Pietro, S. Petralia, S. Conoci, M. Ferrari, L. Cremonesi, Molecular diagnostics on a Lab-on-Chip device. A new advanced solution for mutation detection in gene-diseases, *Clin. Chem. Lab. Med.* 48 (2010) 329–336.

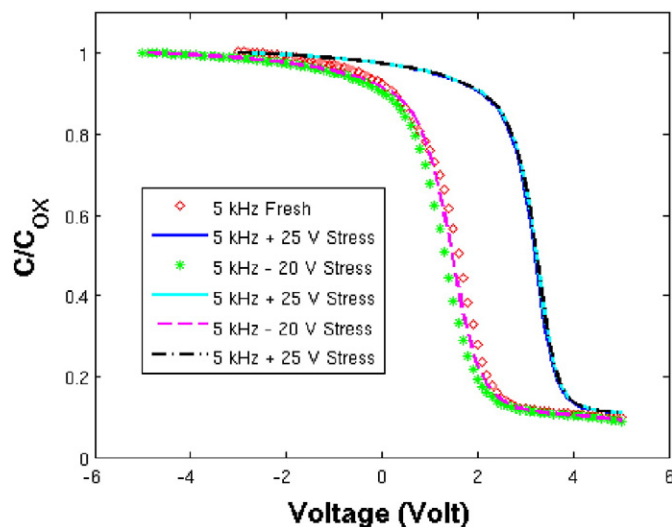


Fig. 8. CV curves of ONO samples as prepared (fresh, red diamonds) and after “programming” (curves blue, light and black dashed fully overlapping) and “erasing” (curves green dotted e magenta dashed and red diamond line) cycles.

- [6] M.F. Santangelo, R. Pagano, S. Lombardo, E.L. Sciuto, D.N. Sanfilippo, P.G. Fallica, F. Sinatra, S. Libertino, Silicon photomultipliers applications to biosensors, Proceeding SPIE 899027, San Francisco, California United States, February 2014.
- [7] G. Korotcenkov, Chemical Sensors Comprehensive Sensor Technologies: Volume 5 Electrochemical and Optical Sensors, Momentum Press, New York, 2012.
- [8] S. Conoci, A. Mascali, F. Pappalardo, Synthesis, DNA binding properties and electrochemistry to an electrode-bound DNA of a novel anthracene-viologen conjugate, RSC Adv. 4 (2014) 2845–2850.
- [9] P. Bataillard, F. Gardies, N. Jaffrezic-Renault, C. Martelet, Direct detection of immunospecies by capacitance measurements, Anal. Chem. 60 (1988) 2374–2379.
- [10] M.J. Schöning, A. Poghosian, Bio FEDs (field-effect devices): state-of-the-art and new directions, Electroanalysis 18 (2006) 1893–1900.
- [11] A. D'Amico, C. Di Natale, E. Martinelli, L. Sandro, G. Baccarani, Sensors small and numerous: always a winning strategy? Sensors Actuators B Chem. 106 (2005) 144–152.
- [12] S. Libertino, S. Conoci, A. Scandurra, R.C. Spinella, Biosensor integration on Si-based devices: feasibility studies and examples, Sensors Actuators B Chem. 179 (2013) 240–251.
- [13] T. Cosentino et al., submitted to applied biosensor surface, 2015
- [14] T. Sakata, M. Kamahori, Y. Miyahara, Immobilization of oligonucleotide probes on Si₃N₄ surface and its application to genetic field effect transistor, Mater. Sci. Eng. C 24 (2004) 827–832.
- [15] S. Libertino, V. Aiello, A. Scandurra, M. Renis, F. Sinatra, S. Lombardo, Feasibility studies of Si-based biosensors, Sensors 9 (2009) 3469–3490.
- [16] B. Eitan, P. Pavan, I. Bloom, E. Aloni, A. Frommer, D. Finzi, NROM: a novel localized trapping 2-bit nonvolatile memory cell, IEEE Electron Device Lett. 21 (2000) 543–545.